

Chemical effects in negative muon capture in some ionic and covalent solids and ionic aqueous solutions*

J. D. Knight, C. J. Orth, and M. E. Schillaci

Los Alamos Scientific Laboratory, Los Alamos, New Mexico 87545

R. A. Naumann

Princeton University, Princeton, New Jersey 08540

H. Daniel and K. Springer

*Los Alamos Scientific Laboratory, Los Alamos, New Mexico 87545
and Technical University of Munich, Munich, Germany[†]*

H. B. Knowles

*Los Alamos Scientific Laboratory, Los Alamos, New Mexico 87545
and Washington State University, Pullman, Washington 99163[†]*

(Received 2 September 1975)

Muonic x-ray spectra have been measured for target sequences including graphite, diamond, their boron-nitride counterparts, three organic compounds, ice and water, eight oxides of metals, alkali halides in aqueous solution and alkali chlorides in anhydrous crystalline form, and calcium and titanium hydrides. Comparisons are made of Lyman-series intensity patterns, and relative muon capture probabilities in the constituent elements of compounds are compared with the "Z-law" relation. The Lyman intensities of the C and N in the low-Z targets are found to exhibit two kinds of pattern, one with relatively weak higher-series members characterizing the diamond and graphite structures, and one with stronger higher-series members characterizing the other (hydrogen-containing) compounds. There is some evidence that the latter intensity behavior applies to the aqueous ions as well. For the oxide sequence, increasing covalency appears to correlate with increasing muon capturing ability of the metal element and with increasing intensity of the higher Lyman members for both the metal element and the oxygen. Effective relative muon-capture cross sections have been obtained for aqueous alkali and halide ions.

I. INTRODUCTION

Experimental studies of the stopping of negative mesons¹ in a variety of substances have shown that the meson capture probabilities and the mesonic-atom x-ray spectra of the constituent elements are affected by their chemical environment.²⁻⁷ Because of instrumental limitations, most of the early investigations dealt with relative capture probabilities. The improvement in energy resolution attained with the development of semiconductor detectors and modern pulse-height analysis systems, however, has added the capability of measuring intensity patterns within x-ray series and has significantly increased the accuracy of the capture measurements as well. Although measurements of this kind have now been made on more than a hundred different materials with negative muons, pions, and kaons, and interesting chemical effects have been observed in several classes of materials, as yet few systematic trends or useful quantitative correlations have emerged, and few empirical rules have been established.

A corresponding situation exists with respect to theoretical analysis. Beginning with the pioneering work of Fermi and Teller⁸ a number of models have been developed,^{2-7,9,10} and the process of meson slowing, capture into bound states, and subsequent deexcitation^{11,12} has been worked out in general outline; however, no existing model satisfactorily explains the observed chemical effects.

We report here the results of some measurements with negative muons aimed at characterizing these chemical effects in simple (or idealizable) systems. Some of our experiments were intended to clarify previously reported trends; others were intended to explore possible trends in system categories selected for variation of the fewest chemical parameters. We have measured muonic x-ray spectra in several groups of low- to medium-Z target materials: solid systems spanning the chemical-bond range from strongly ionic to purely covalent and aqueous solutions of simple ions; in addition, we have examined two metal hydrides, one representing the ionic type and one the interstitial.

II. EXPERIMENTAL PROCEDURES

The experiments were conducted at the stopped muon channel of the Clinton P. Anderson Meson Physics Facility (LAMPF). The accelerator was operated at either 2.5% or 5% duty factor during these runs, and the channel was tuned to deliver (130 ± 5) -MeV/c muons from backward decay of 180-MeV/c pions; the muon beam as used contained ~1% electron contamination and no detectable pions. The beam at the target-center position, as mapped by Polaroid film exposures, was approximately 4 cm wide \times 12 cm high in cross section. Most of our measurements were made at muon stop rates of $3-7 \times 10^4 \text{ sec}^{-1}$ for 3 g/cm^2 of target material measured along the beam axis. Muon stops were detected by a conventional four-element (1234) plastic scintillator telescope. The output signals of the photomultiplier tubes were fed through 23-m-long coaxial cables to the data-processing room, which contained the logic and linear circuitry. Essential features of the target assembly are shown in Fig. 1.

The solid-state targets (except for the graphitic BN and graphite, which were self-supporting) consisted generally of crystalline powders contained in planar Lucite, aluminum, or titanium cells made as U-shaped frames with inner dimensions 17×12 or 17×17 cm and 1 or 2 cm thick, and windows of Mylar, aluminum, or titanium foil, respectively; target thicknesses normal to the window were typically $\sim 2 \text{ g/cm}^2$. The liquid targets were contained in standardized Mylar-windowed Lucite cells 15×15 cm in cross section and 1.5 or 2 cm thick. As indicated in Fig. 1, the targets were oriented at 45° to the muon beam and to the detector. Precautions were taken to insure that the target materials employed were of the highest

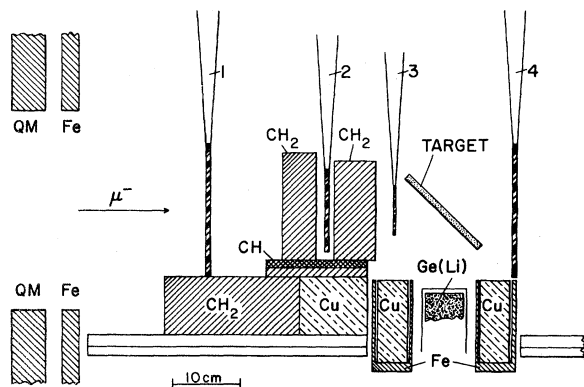


FIG. 1. Target arrangement. Objects 1, 2, 3, and 4 are plastic scintillation counters. QM designates the last quadrupole magnet.

purity practically available. The inorganic salts and oxides were of reagent grade with a purity in excess of 99.5%. The two substituted nitrobenzenes were "Eastman Reagent Chemicals," synthesized by Eastman Kodak Company. The calcium hydride and the titanium hydride were procured from Ventron Corporation, Alfa Products (Beverly, Mass.); the former was reported to be 95% CaH_2 , and the latter 98% TiH_2 . The graphite targets consisted of stacks of machined plates, prepared from pyrolytic graphite stock manufactured by Supertemp Corp. (Santa Fe Springs, Calif.); total ash content was reported to be less than 0.01%. The graphitic boron nitride was machined from Union Carbide Corporation HBR-Grade stock that had been furnace-roasted prior to machining. The cubic (i.e., diamond-like) forms of carbon and boron nitride were manufactured by the General Electric Company Specialty Materials Department and are marketed under the trademarks "Man-Made" diamond and "Borazon," respectively; they were used as received.

We detected the muonic x-rays with either of two detectors, depending on the energy range of interest: for the low- Z target series (B, C, N, and O) a 38-mm-diam \times 12-mm-thick planar intrinsic Ge unit; for all the others, including oxides of the higher- Z elements, a 70-cc closed-end coaxially drifted Ge(Li) unit. In typical use during accelerator operation, both detectors had resolutions of ~ 1.5 keV at 122 keV. Pulse-height spectra were measured and stored in a 4096-channel pulse-height analyzer employing a 100-MHz analog-to-digital converter. In the case of the oxides and aqueous solutions, for which the large Ge(Li) detector had to be used, the very large range of x-ray energy and the corresponding range in detector preamplifier pulse size created problems with detector pulse timing and overall electronic efficiency of the detector/scintillator telescope coincidence system. The solution chosen was to set the coincidence time gate of this system relatively wide, at 80 nsec, and then to take into account the lost pulses by empirically measuring the relative coincidence efficiency as a function of x-ray energy from a comparison of singles and coincidence-gated muonic x-ray spectra. Target materials used for the comparison spectra were Y_2O_3 (97–2430 keV), NaKCO_3 (133–712 keV), and NaCl (250–578 keV).

Detector photopeak efficiency functions, including off-axis positions, were determined to 1.8 MeV with NBS-calibrated sources, and thence to 10 MeV (for the large detector) by fitting the relative efficiency function obtained by measuring the γ spectrum from $^{14}\text{N}(n, \gamma)^{15}\text{N}$. Absorption coefficients for the muonic x-rays in the targets were determined

by measuring, for each target as used, the attenuations of a series of γ standards covering the energy range of interest. Absorption plus extended source corrections were then calculated with a Los Alamos computer code. Photopeak intensities in the muonic x-ray spectra were generally extracted with a version of the GAMANAL code,¹³ which fits each peak in terms of a Gaussian plus a low-energy-side exponential. The fitting routine did not adapt well to measuring broadened peaks; in these cases it was necessary to supplement the fitting routine by "hand" integration.

One objective of our experiment was the determination of the relative muon atomic capture probabilities $W(Z)$ and $W(Z')$ for the elements Z and Z'

in the compound $Z_m Z'_k$. We follow the convention employed by Ponomarev⁴ and by the CERN-Munich group¹⁴ in defining an atomic capture ratio as

$$A(Z/Z') = \frac{W(Z)/m}{W(Z')/k},$$

the capture ratio per atom. We evaluated $W(Z)$ and $W(Z')$ by the general procedure of summing the intensities of all observed Lyman-series transitions. Within the limits of accuracy of present-day measurements, each muon captured in one of the elements studied in this work must undergo one of these transitions.¹¹ For elements with $Z \geq 20$ this procedure amounted to truncating the summation at about the $K\epsilon$ member, beyond which the

TABLE I. Muonic x-ray data, low- Z targets.

Intensity ratio ($\times 10^3$)	Lyman intensity patterns					
	C diamond	C graphite	(CH ₂) _n	CH ₃ - \ominus -NO ₂	Cl- \ominus -NO ₂	C ₃ H ₇ OH
Carbon						
$K\beta/K\alpha$	267 \pm 20	290 \pm 20 (305 \pm 19) ^a	426 \pm 30 (383 \pm 33) ^b	427 \pm 30	404 \pm 30	(438 \pm 16) ^c
$K\gamma/K\alpha$	137 \pm 13	138 \pm 13 (135 \pm 10) ^a	262 \pm 25 (222 \pm 23) ^b	235 \pm 25	211 \pm 25	(230 \pm 10) ^c
$K\nu/K\alpha$	39 \pm 10	48 \pm 10	68 \pm 14	63 \pm 15	55 \pm 15	(76 \pm 5) ^c (23 \pm 4) ^c
Boron						
$K\beta/K\alpha$	BN diamond	BN graphite				
$K\nu/K\alpha$	312 \pm 20 (170)	305 \pm 20 168 \pm 12				
Nitrogen						
$K\beta/K\alpha$	266 \pm 20	278 \pm 20		354 \pm 24	345 \pm 24	
$K\gamma/K\alpha$	160 \pm 13	166 \pm 16		252 \pm 20	225 \pm 20	
$K\delta/K\alpha$	60 \pm 12	57 \pm 12		
$K\nu/K\alpha$	26 \pm 15	58 \pm 15		80 \pm 25	72 \pm 20	
Oxygen						
$K\beta/K\alpha$	Ice	Water				
$K\gamma/K\alpha$	305 \pm 12	302 \pm 12 (270 \pm 8) ^a		300 \pm 20	326 \pm 20	(324 \pm 14) ^c
$K\delta/K\alpha$	252 \pm 12	248 \pm 12 (221 \pm 8) ^a		260 \pm 20	254 \pm 20	(302 \pm 13) ^c
$K\nu/K\alpha$	123 \pm 9	126 \pm 9 (108 \pm 7) ^a		116 \pm 20	139 \pm 20	(150 \pm 9) ^c
	57 \pm 8	50 \pm 8 (36 \pm 5) ^a		30 \pm 9	30 \pm 9	(35 \pm 5) ^c
Z-law data						
$\Sigma B/\Sigma N$ meas.	BN diamond	BN graphite				
Z-law	0.235 \pm 0.020	0.258 \pm 0.020				
$\Sigma C/\Sigma N$ meas.				5.79 \pm 0.40	4.81 \pm 0.35	
Z-law				6.00	5.14	
$\Sigma O/\Sigma N$ meas.				2.67 \pm 0.14	2.78 \pm 0.14	
Z-law				2.286	2.286	
$\Sigma C/\Sigma O$ meas.				2.17 \pm 0.15	1.73 \pm 0.13	
Z-law				2.625	2.250	

^a Ref. 15.^b Ref. 16.^c Ref. 18.

intensities were too low for detection. On the basis of cascade calculations we estimate that this truncation introduces an error of the order of a few percent.

In the evaluation of the capture ratios $A(Z/O)$ for the oxides of the medium- Z elements (Sec. III B) and for the aqueous solutions of the metal halides (Sec. III C) an additional uncertainty is introduced in determining the relative coincidence efficiency for the muonic K x rays from oxygen ($E \sim 140$ keV), which lie at the low-energy end of the spectrum measured. Here we estimate the error in determining the coincidence efficiency as no larger than $\pm 10\%$. Combining this with an estimated $\pm 4\%$ error in the relative intrinsic efficiency of the Ge(Li) detector for the two relative K photon groups, we identify an additional uncertainty of approximately $\pm 11\%$ beyond the statistical errors shown in the $A(Z/O)$ entries of Tables II and III.

III. RESULTS AND DISCUSSION

A. Covalent molecules of low- Z elements

Our first measurements involved targets of simple molecules containing boron, carbon, nitrogen, and oxygen, and were intended to explore the effects of bond type and symmetry and of charge displacement on the mesonic x-ray spectra. The bonds in the molecules chosen are predominantly covalent and the structures are believed to be well understood. It might be expected that the chemical effects should be most prominent where there are fewest electrons per atom; in carbon, for example, four of the six electrons participate directly in chemical bonds. Three of the target materials in our selection had been measured previously by other investigators and were included in our list for comparison purposes. Our results are summarized in Table I. We comment on individual comparisons in the following paragraphs.

(a) *Water/ice*. The basic question in this experiment was whether a change from liquid to crystalline lattice, without radical electronic rearrangement, would produce a detectable difference in the muonic x-ray spectrum of the oxygen. (The corresponding transitions in hydrogen were too low in energy for measurement in our system). The water was measured at 20°C and the ice at melting temperature (0°C). As may be seen from the Lyman intensity patterns, the two spectra were identical within experimental error. Earlier data¹⁵ for water are in fair agreement with ours, although about at the limits of the errors cited.

(b) *Graphite and diamond forms of C and BN*. Here we examine two effects: The influence of a change in bond type and symmetry on the Lyman intensity pattern, and the effect of charge displacements on

the capture ratio for BN. We observe first that for carbon, as for both the boron and nitrogen in BN, the Lyman intensity patterns are essentially the same in the diamond and in the graphitic forms. Second, we observe that the B/N capture ratio deviates sharply from the " Z Law"—about a factor of 3 in favor of the N—whereas the C/N and O/N ratios in the other nitrogen-containing compounds measured lie within $\sim 20\%$ of the Z law. The deviation in the case of BN, one of the largest of which we are aware in low- Z compounds, may be associated with electron displacement in the B-N bond. As yet, we know of no method for calculating the magnitude of this effect. We do note, however, the similarity with the large muon capture probability observed for the oxygen in the isoelectronic compound BeO ,¹⁷ where the oxygen is describable as an O^{2-} ion. This suggests that the nitrogen atoms in BN could have a net *negative* charge instead of a positive charge as commonly depicted.

In selecting sets of target materials of this kind to represent certain idealized bond types one unavoidably encounters variations in other properties, such as electrical conductance and band gap, which may affect the mesonic properties measured. However, the similarity in muonic Lyman-intensity patterns for the two forms of carbon and BN indicate that the effects must be small relative to those produced by other changes in molecular structure.

(c) *Organic compounds*. We list in this section three organic compounds representing certain structural features: polyethylene typifying long-chain hydrocarbons, nonpolar, and two para-substituted nitrobenzenes, with the para-substituents chosen to differ widely in their inductive influence on the nitro group (dipole moments of the two compounds differ by $\sim 2.0\text{D}$). For additional comparison we list also data for propyl alcohol from d'Oliveira, Daniel and von Egidy.¹⁸

Examination of the data in Table I for all carbon-containing materials reveals an interesting feature: the Lyman intensity patterns fall into two families, one for graphite and diamond (with $K\beta/K\alpha \approx 0.28$) and the other for all the other carbon compounds (with $K\beta/K\alpha \approx 0.42$). Intensity-pattern differences within the latter family are small and perhaps real, but they are overshadowed by the great difference between the two families. The same division, to a lesser degree, is seen to occur for nitrogen; again, it is the diamondlike and graphitelike compounds that exhibit the smallest $K\beta/K\alpha$. Are there any obvious structural characteristics that distinguish the diamond and graphite and their BN counterparts from the other molecules? We note that there are two: the elec-

tron distributions around the C and N in the other molecules are more asymmetric, and the other molecules contain hydrogen; although the nitrogen in the nitro compounds is not bonded directly to hydrogen, the N-H distance in the free molecule is not great and in the condensed phase (the target form we used) intermolecular packing may bring N-H distances to nearly normal bond length. We are unable to ascertain with certainty at this time which of the two effects is predominantly responsible for the increased intensity of the higher Lyman members: the increased asymmetry in binding, the presence of (bound) hydrogen, or neither. We point out, however, that the local tetrahedral bonding symmetry about the carbon in diamond is approximately reproduced in polyethylene. This fact, together with our data for the aqueous ions (Sec. III C), leads us to the tentative suggestion that the observed intensity variation is due to the presence of hydrogen. A few simple critical experiments now being planned should resolve this question.

In the two nitro compounds, the aromatic ring may be considered mainly as a structural member and as a conduit for movement of negative charge to or from the nitro group (the *para*-CH₃ and *para*-Cl compounds, respectively). From the difference in dipole moments of the two molecules, one may estimate that in the *para*-CH₃ case of the order of 0.1 additional electron charge has moved to the two oxygens. Although this represents an effective increase of less than 1% in their electron inventory, we wished to determine whether an inductive effect of this magnitude would be visible in the mesonic x-ray spectra. As may be seen from Table I, it is not. Within our limits of experimental error, the N and O Lyman intensity patterns and the N/O capture ratios appear to be identical.

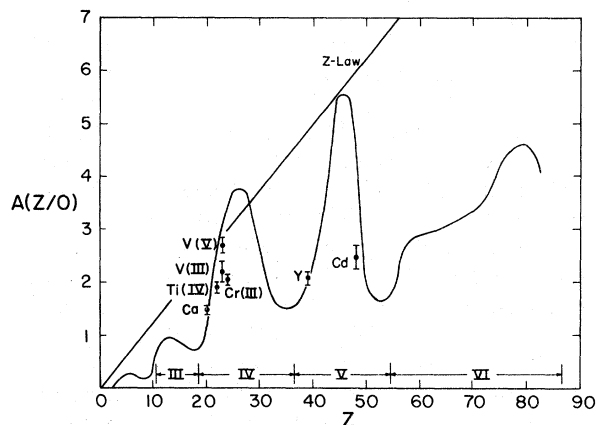


FIG. 2. Relative capture of muons per atom of the element Z in oxides. Points represent our data; the smooth curve indicates the trend as sketched by Zinov *et al.* (Ref. 17).

B. Metal oxides

Our interest in the oxide targets was prompted by the well-known paper of Zinov *et al.*,¹⁷ who noted that the relative capture of muons per atom of the element Z in the oxide Z_mO_k ,

$$A(Z/O) = \frac{W(Z)/m}{W(O)/k},$$

for a series of oxides was not a monotonic function of Z but appeared to vary in an oscillatory fashion that correlated with the periodic table of the elements. [Note: the quantity we define as $A(Z/O)$ was designated $W(Z)/W(O)$ by Zinov *et al.*] Our purpose was to explore further this variation. In order to examine the influence of bond ionicity patterns we compared muonic x-ray spectra of the series V_2O_3 , V_2O_4 , V_2O_5 . Our results are shown

TABLE II. Muonic x-ray data, metal oxides.

Oxide	Lyman intensity ratios ($\times 10^3$)				Metal			Oxygen			Capture ratio	
	$K\beta/K\alpha$	$K\gamma/K\alpha$	$K\delta/K\alpha$	$K\epsilon/K\alpha$	$K\beta/K\alpha$	$K\gamma/K\alpha$	$K\nu/K\alpha$	$K\beta/K\alpha$	$K\gamma/K\alpha$	$K\nu/K\alpha$	Expt.	Z-law
CaO	79 \pm 13	29 \pm 10	18 \pm 6	19 \pm 6	...	100 \pm 30	38 \pm 13	1.45 \pm 0.09 ^a	2.50			
TiO ₂	78 \pm 17	29 \pm 10	30 \pm 11	28 \pm 12	257 \pm 40	178 \pm 30	123 \pm 16	1.90 \pm 0.10	2.75			
V ₂ O ₃	86 \pm 16	49 \pm 18	38 \pm 13		250 \pm 50	200 \pm 40	140 \pm 40	2.19 \pm 0.18	2.88			
V ₂ O ₄	96 \pm 15	44 \pm 10	37 \pm 11		310 \pm 50	200 \pm 30	150 \pm 20	2.28 \pm 0.23	2.88			
V ₂ O ₅	100 \pm 11	43 \pm 10	40 \pm 10		260 \pm 40	190 \pm 30	140 \pm 20	2.68 \pm 0.14	2.88			
Cr ₂ O ₃	115 \pm 18	61 \pm 28	56 \pm 17		344 \pm 53	251 \pm 37	138 \pm 29	2.04 \pm 0.11	3.00			
Y ₂ O ₃	52 \pm 13	13 \pm 8			221 \pm 19	146 \pm 16	89 \pm 15	2.07 \pm 0.13	4.88			
CdO	52 \pm 26				357 \pm 40 ^b	153 \pm 46 ^b		2.47 \pm 0.22	6.00			

^a Oxygen $K\beta$ could not be resolved from strong calcium $L\alpha$. In the evaluation of $A(\text{Ca}/\text{O})$, $K\beta/K\alpha=0.257$ (from TiO_2) was used.

^b These lines may contain contributions from the cadmium M series.

in Table II, which lists the intensity ratios $K_i/K\alpha$ ($i = \beta, \gamma, \delta, \epsilon, \nu$) for the Lyman series of the elements and the oxygens, and also the capture ratios. Missing entries in the Lyman intensity listings of the elements are cases where the corresponding x-ray-spectrum photopeaks were too weak to resolve from background. The capture ratios $A(Y/O)$ and $A(Cd/O)$ are estimated to be $\sim 2\%$ and $\sim 5\%$ low, respectively, due to undetected Lyman lines. In the cases (CaO, TiO₂, V₂O₄, Y₂O₃) where the oxide samples were contained in Lucite, a correction was applied for the oxygen intensity contributed by the container.

From an examination of Table II and Fig. 2 we note first of all that our capture-probability results are consistent with the periodic trend reported by Zinov *et al.*,¹⁷ but more data are needed before we can confirm this trend. We note also that the Lyman intensity patterns for both the element Z and the oxygen vary with position of the element within its period. In general, progression through the series of oxides from strongly ionic (CaO) to strongly covalent (V₂O₅) is accompanied by increasing strength of the higher members of the Lyman spectrum.

Au-Yang and Cohen¹⁹ took account of the correlation between the periodic behavior of $A(Z/O)$ for the oxides as reported by Zinov *et al.*¹⁷ and the electronegativities of the elements as tabulated by Pauling,²⁰ and formulated an interpretation of the $A(Z/O)$ variation in terms of an "effective

charge" parameter associated with the atom combined with oxygen. This parameter, labeled Z_f , is defined as the product of the number of valence electrons in the common oxidation state and the ionic character of the bond, the latter being given by Pauling in terms of the difference in electronegativities of the two atoms (or ions) participating in the bond.

An examination of our oxide data confirms the correlation noted above; in addition it permits the illustration of a simple relationship between $A(Z/Z')$ and Pauling's electronegativities (χ) of the elements oxidized. In Fig. 3 we plot $A(Z/Z')/(Z/Z')$ vs χ/Z for the oxides and also for the chlorides. (The division by Z in ordinate and abscissa scales has been done only to permit a clearer display of the data). As may be seen, the points for the oxides show a smooth interdependence between atomic capture and electronegativity. A similar situation exists for the chlorides.

C. Alkali halides

In comparing the meson capture characteristics of a given element when chemically combined in various compounds, we encounter two possible complications. The electronic structure of the element in question and its environment will vary from compound to compound, and the energy spectrum of the mesons in the medium and thus of the mesons captured may differ also from compound to compound. Dilute solutions, such as aqueous solutions of simple salts, offer the possibility of a partial simplification of this problem; the energy spectrum of the captured mesons should be relatively constant and determined by the solvent (in this case water), and we can study the capture properties of individual ions located in a uniform medium. The water, of course, also performs the additional important function of dispersing the solute material by electrolytic dissociation into individual ions, each enclosed in a hydration sphere.

For our investigation we chose a series of solutions of alkali halides. On the basis of the considerations outlined above, we expected that for a given ionic species the muonic x-ray intensity pattern and muon capture probability per unit concentration should be constant. We also investigated three of these salts (NaCl, KCl, and RbCl) in crystalline form both for comparison with our observations on the aqueous solutions and to examine the Z dependence of the capture ratios reported by Zinov *et al.*¹⁷ for this class of compounds.

(a) *Aqueous solutions.* For most of our measurements we adopted a salt concentration of $2M$

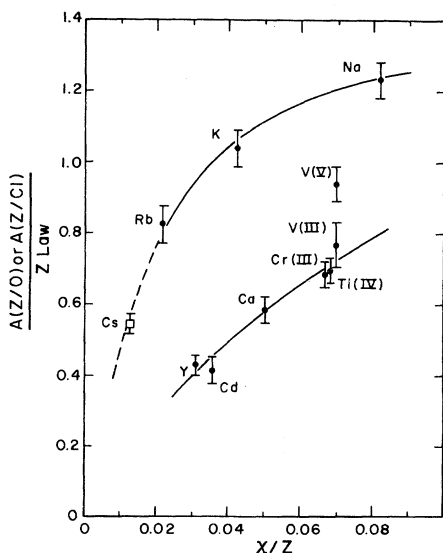


FIG. 3. Relative capture of muons per atom of the element Z in oxides and chlorides as a function of electronegativity. The horizontal scale is the electronegativity as tabulated by Pauling (Ref. 20) divided by atomic number.

TABLE III. Relative muon capture probabilities for simple aqueous ions.

Solution	$10^4 \frac{W_\alpha(M^+)}{W(O)}$ ^a	$10^4 \frac{W_\alpha(X^-)}{W(O)}$ ^a	$m(\text{salt})$ ^b	$c(\text{H}_2\text{O})$ ^b	Capture probability per atom relative to oxygen			
					$A(M^+_\alpha/O)$	$A(\text{Cl}^-_\alpha/O)$	$A(\text{Br}^-_\alpha/O)$	$A(I^-_\alpha/O)$
2.00M NaCl	211±19	424±39	2.08	55.5	0.56±0.05	1.13±0.10		
4.00M NaBr	399±28	1043±63	4.49		0.49±0.04		1.29±0.08	
2.00M KF	252±28	... ^c	2.05		0.68±0.07			
2.00M KCl	352±47	358±30	2.13		0.92±0.12	0.93±0.08		
4.00M KBr	684±69	696±36	4.57		0.83±0.08	0.84±0.04		
2.00M (KBr)	320±23	561±34	2.16		0.82±0.06		1.44±0.09	
2.00M KI	338±54	675±116	2.21		0.85±0.14			1.69±0.29
1.00M CaCl ₂	209±30	398±30	1.03		1.13±0.16	1.07±0.08		
1.81M RbCl	450±47	367±52	1.94		1.29±0.13	1.05±0.15		
1.76M CsCl	552±79	365±40	1.91		1.61±0.23	1.06±0.12		

^a $W_\alpha(M^+)$, $W_\alpha(X^-)$ = M^+ , X^- $K\alpha$ intensity; $W(O)$ = total $O K$ intensity.

^b m = molal concentration = (moles of solute)/1000 g of H_2O ; c = molal concentration of pure H_2O .

^cFluorine $K\alpha$ was obscured by oxygen $K\gamma$.

(2 moles per liter of solution). This choice represented a compromise between the desiderata of large dilution and reasonable muonic x-ray intensity of the ions. The oxygen Lyman series from the water served as the internal reference for evaluation of the ionic capture probabilities. Intensity patterns for the mesonic K x-rays from the aqueous ions were limited to observation of the α and β members due to the lower contributions from these elements in the overall spectra. The capture-probability data are given in Table III. The constancy of the muon capture probability for a given ionic species (independent of the counter ion) is revealed by the entries for Na^+ , K^+ , Cl^- , and Br^- . The 2M- and 4M- solution data provide a limited test of the concentration independence of these capture probabilities. The Z dependence

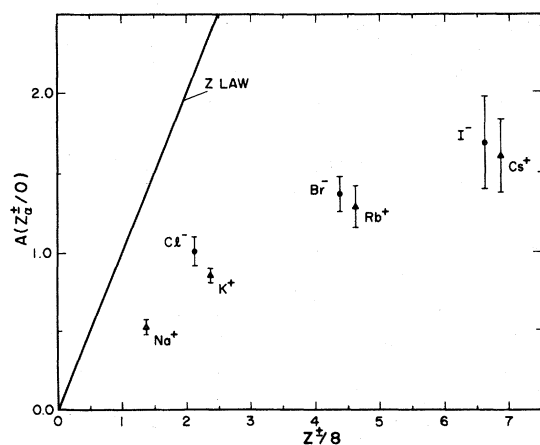


FIG. 4. Muon atomic capture ratio $A(Z^+_\alpha/O)$ for aqueous ions relative to the oxygen of water. The straight line represents the Z -law relation.

of the aqueous-ion capture probabilities is illustrated in Fig. 4; we see that the negative ions are slightly more effective in capturing muons than are the positive ions, and that the capture probabilities do not appear to follow any single power of Z .

(b) *Crystalline alkali chlorides.* The muonic Lyman intensity patterns of the crystalline NaCl, KCl, and RbCl are listed in Table IV. Our data for NaCl and KCl are in general agreement with recently reported values.^{14,21} The intensity patterns for the Cl^- ions in the three salts are the same within experimental error, in agreement with the observations in Ref. 21. Also included in

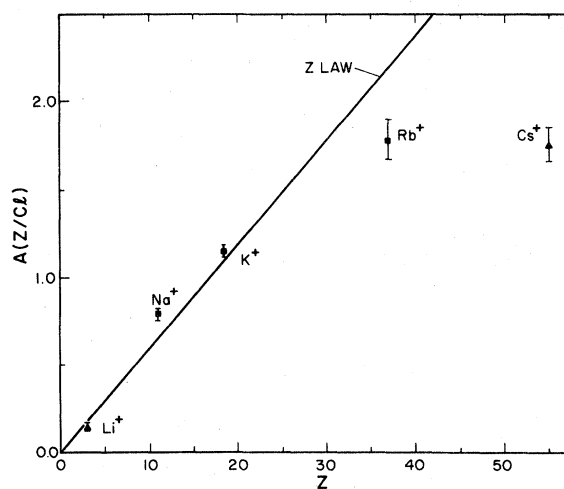


FIG. 5. Muon atomic capture ratio $A(Z/\text{Cl})$ as a function of Z for crystalline alkali-halide salts. The points for lithium chloride and cesium chloride (marked by triangles) are taken from the work of Bobrov *et al.* (Ref. 22). The straight line represents the Z -law relation.

TABLE IV. Muonic x-ray data, alkali chlorides.

Chloride	Lyman intensity ratios ($\times 10^3$)							Capture ratio	
	Alkali element			Chlorine				$A(Z/Cl)$	
	$K\beta/K\alpha$	$K\gamma/K\alpha$	$K\delta/K\alpha$	$K\beta/K\alpha$	$K\gamma/K\alpha$	$K\delta/K\alpha$	$K\epsilon/K\alpha$	Expt.	Z-law
LiCl ^a								$0.139^{+0.025}_-0.019$ ^a	0.176
NaCl	98 \pm 12	59 \pm 11	31 \pm 8	71 \pm 11	22 \pm 6	18 \pm 6		0.787 \pm 0.031	0.647
KCl	52 \pm 10	37 \pm 9		76 \pm 12	31 \pm 12			1.15 \pm 0.05	1.12
RbCl	56 \pm 15			75 \pm 15	32 \pm 13	22 \pm 7	24 \pm 10	1.78 \pm 0.11	2.18
CsCl ^a								1.75 \pm 0.09 ^a	3.24

^a Ref. 22.

the table are the capture ratios for LiCl and CsCl reported by Bobrov *et al.*,²² as well as the Z-law ratios. In Fig. 5 we show a plot of $A(Z/Cl)$ vs Z . It is clear that the simple linear Z dependence suggested by Zinov *et al.*¹⁷ is not adequate. Our capture-ratio data are in accord with those of Refs. 14 and 21.

(c) *Lyman intensity comparisons of crystalline and aqueous ions.* It is of interest to compare the Lyman intensity patterns of the crystalline ions with those of their aqueous counterparts, which are sheathed in water molecules. Relevant $K\beta/K\alpha$ ratios are shown in Table V. For solutions the expected constancy of the $K\beta/K\alpha$ intensity ratio is best demonstrated by the aqueous Cl^- ion; we find an average value $K\beta/K\alpha = 0.13 \pm 0.03$. The corresponding ratio for the crystalline chlorides is 0.075 ± 0.003 . The $K\beta/K\alpha$ ratios for the aqueous Na^+ and K^+ ions also appear constant within the larger quoted errors. It is of interest to note that for the aqueous chloride ion and probably for all the aqueous ions the $K\beta/K\alpha$ ratio is higher than for the same ion in the crystalline state. It has been noted that for muon capture in hydrogenous chemical compounds²³ or for mixtures containing hydrogen²⁴⁻²⁶ similar intensity characteristics

are exhibited, and we suggest that the hydrogen atoms in the vicinity of the aqueous ions may account for the enhancement of the $K\beta/K\alpha$ intensity ratios.

D. Hydrides

Previous investigators^{24, 25} have shown that when negative muons are captured in argon gas which has been greatly diluted by hydrogen (of the order of 10^{-1} – 10^{-3} at. % Ar), such that most of the captures in argon occur by way of the intermediate "pseudoneutron" $p\cdot\mu$, the intensities of higher members of the muonic Lyman series are strongly enhanced relative to their intensity in pure argon. Hartmann *et al.*²⁶ have observed intensity differences in comparisons of the higher muonic x-ray lines from pure niobium and from the hydrogen-impregnated form $NbH_{0.93}$; the latter is considered to have its hydrogen in lattice interstices in an "unbonded" form. These measurements could be interpreted in a manner similar to those of the Ar/Ar-H₂ comparison. The same effect could also occur in compounds containing chemically bonded hydrogen, but it is commonly supposed (as proposed in extensive studies by Soviet inves-

TABLE V. Comparison of $K\beta/K\alpha$ intensity ratios for alkali halides in aqueous solution and crystalline state.

Ion	Solution	$K\beta/K\alpha$ (10^{-3})	Crystal	$K\beta/K\alpha$ (10^{-3})
Na^+	2M NaCl	212 \pm 104	NaCl	98 \pm 12
	4M NaBr	111 \pm 45	NaCl	(100 \pm 11) ^a
K^+	4M KCl	105 \pm 32	KCl	52 \pm 10
	2M KBr	179 \pm 31	KCl	(73 \pm 4) ^a
Cl^-	2M NaCl	131 \pm 49	NaCl	71 \pm 11
	2M KCl	158 \pm 76	NaCl	(73 \pm 4) ^a
	4M KCl	150 \pm 34	KCl	76 \pm 12
	1M CaCl ₂	95 \pm 43	KCl	(81 \pm 5) ^a
	1.81M RbCl	156 \pm 52	CaCl ₂	(73 \pm 3) ^a
	1.76M CsCl	79 \pm 29	RbCl	75 \pm 15

^a Ref. 21.

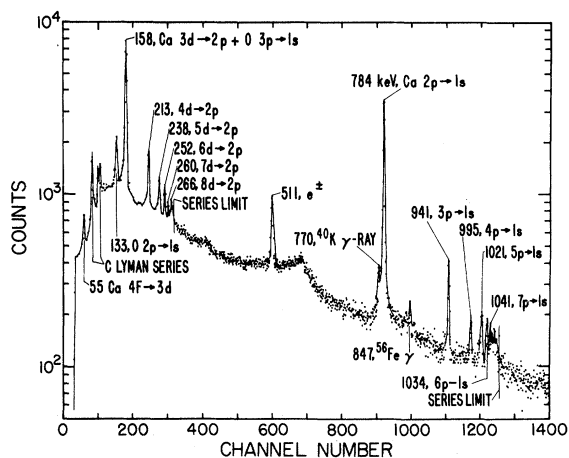


FIG. 6. Muonic x-ray spectrum of CaH_2 , measured with the large $\text{Ge}(\text{Li})$ detector.

tigators^{2,4,5}) that so few mesons are captured by the bound hydrogen in the first place—typically 10^{-2} – 10^{-3} of the Z -law prediction—that their contribution to the overall mesonic x-ray spectrum of the other elements via the transfer mechanism would be below detectability limits.

As part of our series of experiments we sought to determine whether the hydrogen effect could be seen in solid targets by comparing mesonic Lyman and Balmer spectra of CaH_2 (containing bound hy-

drogen) and TiH_2 (containing unbonded hydrogen, like the NbH). The mesonic x-ray spectrum observed for CaH_2 is shown in Fig. 6. Our results are summarized in Table VI, where we compare the mesonic x-ray intensity patterns of the two hydrides and also of the oxides CaO and TiO_2 , and titanium-metal data reported by Kessler *et al.*²⁷ and the calcium-metal data reported by Mausner *et al.*²¹ As may be seen, neither hydride shows a marked enhancement of the higher members of the K and L series relative to the pattern in the corresponding oxides. The apparent lack of a hydrogen effect in the Lyman and Balmer series may, of course, simply stem from Z considerations. If the Z law holds approximately for the Ti-H “mixture,” only about 10% of the muons would have been captured initially in H and thus have been available for transfer to Ti atoms. Assuming an effect comparable to that for Ar, the contribution of the $\mu\cdot p$ intermediate should have produced a change in $K\beta/K\alpha$ of about only 0.017.

IV. CONCLUSIONS

From a consideration of the experimental data for the low- Z elements (summarized in Table I) we consider that the salient feature is the appearance of two distinct Lyman-series intensity patterns for both carbon and nitrogen. The diamond and graphitic modifications of carbon as well as

TABLE VI. Muonic Lyman and Balmer intensities in Ca and Ti.

Intensity ratio ($\times 10^3$)	CaH_2	CaO	Ca metal ^a	TiH_2	TiO_2	TiO_2^b	Ti metal ^b
$\frac{3p \rightarrow 1s}{2p \rightarrow 1s}$	91 ± 10	79 ± 13	79 ± 3	87 ± 10	78 ± 11	93 ± 6	102 ± 3
$\frac{4p \rightarrow 1s}{2p \rightarrow 1s}$	25 ± 6	29 ± 10	25 ± 2	37 ± 8	29 ± 10	27 ± 5	31 ± 4
$\frac{5p \rightarrow 1s}{2p \rightarrow 1s}$	34 ± 7	18 ± 6	25 ± 2	25 ± 6	30 ± 11	25 ± 5	36 ± 3
$\frac{6p \rightarrow 1s}{2p \rightarrow 1s}$	23 ± 6	19 ± 6	23 ± 2	31 ± 6	28 ± 12	28 ± 5	41 ± 3
$\frac{7p \rightarrow 1s}{2p \rightarrow 1s}$	14 ± 4	10 ± 4	15 ± 2	23 ± 4
$\frac{4d \rightarrow 2p}{3d \rightarrow 2p}$	154 ± 21	... ^c	109 ± 16	140 ± 16	157 ± 18	151 ± 6	180 ± 6
$\frac{5d \rightarrow 2p}{3d \rightarrow 2p}$	67 ± 10	...	46 ± 6	54 ± 9	54 ± 10	73 ± 6	99 ± 3
$\frac{6d \rightarrow 2p}{3d \rightarrow 2p}$	54 ± 9	...	25 ± 4	42 ± 8	38 ± 12	51 ± 6	81 ± 4
$\frac{7d \rightarrow 2p}{3d \rightarrow 2p}$	18 ± 5	...	16 ± 4	21 ± 6	18 ± 8

^aRef. 21.

^bRef. 27.

^cCa Balmer ratios for CaO were not calculated because Ca $L\alpha$ line at 158 keV could not be resolved from strong O $K\beta$ line.

the corresponding forms of boron nitride provide examples of carbon and nitrogen muonic K x-ray series in which the intensities of the higher members are reduced relative to those for polyethylene, propyl alcohol, and the two substituted nitrobenzenes. As we have pointed out, these two groups of compounds differ in two respects: The local symmetry of the bond structure around the C and N atoms is lower in the second group of compounds than in the first, and all members of the second group contain hydrogen. The presence of hydrogen in a compound is most probably the decisive factor in the enhancement of the higher-series members, since such an enhancement is known to occur when Coulomb capture takes place by transfer from the neutral system $\mu \cdot p$.^{24, 25, 28} In this respect we point out that for the nitrogens in the substituted nitrobenzenes the high-member enhancement also is exhibited, consistent with the transfer mechanism, even though no hydrogens are directly bonded to the nitrogens. The higher $K\beta/K\alpha$ intensity ratios we observe for the aqueous ions (Table V) also support this suggestion. This hypothesis will be tested by experiments now in preparation in which comparison will be made between carbon and nitrogen compounds with a variety of geometries and hydrogen contents.

The effects of phase change and allotropy on muonic x-ray spectra have been investigated. We observed no significant differences in the K x-ray patterns between water and ice or between the diamond and graphite forms of either carbon or boron nitride. For the fourth- and fifth-period metal oxides tested, increasing covalency appears to correlate with increased relative intensity of the

higher members of the Lyman series for both the constituent elements. We also confirm for these oxides the previously reported periodic variation in the muon capture ratio $A(Z/O)$.

For the crystalline alkali-metal chlorides we find that the muon atomic capture ratio $A(Z/Cl)$ increases smoothly with Z . From a study of muon capture by aqueous solutions of alkali halides we have obtained effective relative capture cross sections for the individual aqueous ions, independent of concentration and counter ion. These cross sections provide a basis for nondestructive analysis of solutions of chemical or biological interest using muons.

ACKNOWLEDGMENTS

We wish to express our gratitude to Dr. D. C. Hagerman and the accelerator operating team of LAMPF for their support and cooperation, to Dr. P. A. Thompson for his willing contribution of talent and effort to the successful setup, management, and maintenance of the muon channel system, and to Dr. J. E. Sattizahn and the staff of the Nuclear Chemistry Group for their essential support throughout the course of this work. We also thank the General Electric Company for the generous loan of the synthetic diamond and of the tetrahedral form of boron nitride used in this work. Two of us (H. D. and K. S.) wish to thank the staff of the facility, and in particular Dr. L. Rosen and Dr. E. A. Knapp, for the kind hospitality they received during their stay at Los Alamos. Two of us (H.B.K. and R.A.N.) record their appreciation of the many kindnesses shown them during sabbatical leaves at Los Alamos.

*Work performed under the auspices of the U.S. Energy Research and Development Administration.

†Permanent address.

¹In this paper we employ the older usage according to which a "meson" is a particle of intermediate mass, e.g., a muon, pion, or kaon. Since the chemical effects of interest here involve only the electromagnetic interaction, we prefer to use a single generic term rather than to complicate our terminology with distinctions based on the other interactions.

²S. S. Gershtein, V. I. Petrukhin, L. I. Ponomarev, and Yu. D. Prokoshkin, *Usp. Fiz. Nauk* **97**, 3 (1969) [*Sov. Phys. Usp.* **12**, 1 (1969)].

³Y. N. Kim, *Mesic Atoms and Nuclear Structure* (American Elsevier, New York, 1971).

⁴L. I. Ponomarev, *Ann. Rev. Nucl. Sci.* **23**, 395 (1973).

⁵L. I. Ponomarev, in *High-Energy Physics and Nuclear Structure — 1975 (Santa Fe and Los Alamos)*, AIP Conf. Proc. No. 26, edited by D. E. Nagle, A. S. Goldhaber, C. K. Hargrove, R. L. Burman, and B. G. Storms

(American Institute of Physics, New York, 1975).

⁶S. S. Gershtein and L. I. Ponomarev, in *Muon Physics*, edited by V. W. Hughes and C. S. Wu (Academic, New York, 1975), Vol. 3, Chap. VII, Sec. 2.

⁷V. S. Evseev, in Ref. 6, Vol. 3, Chap. VII, Sec. 3.

⁸E. Fermi and E. Teller, *Phys. Rev.* **72**, 399 (1947).

⁹M. Leon and R. Seki, *Phys. Rev. Lett.* **32**, 132 (1974).

¹⁰P. K. Haff, P. Vogel, and A. Winther, *Phys. Rev. A* **10**, 1430 (1974).

¹¹Y. Eisenberg and D. Kessler, *Nuovo Cimento* **19**, 1195 (1961); *Phys. Rev.* **123**, 1472 (1961).

¹²J. Hüfner, *Z. Phys.* **195**, 365 (1966), and computer program CASCADE (CERN, Geneva).

¹³J. B. Niday and R. Gunnink, University of California Lawrence Radiation Laboratory Report UCRL-51061 (unpublished); modified and transcribed for use at Los Alamos by B. R. Erdal and W. A. Sedlacek.

¹⁴A. B. d'Oliveira, H. Daniel, and T. von Egidy (unpublished).

¹⁵H. Koch, Ph.D. thesis (University of Karlsruhe, 1969),

- as cited by A. B. d'Oliveira, H. Daniel, and T. von Egidy, *Nuovo Cimento Lett.* **10**, 197 (1974).
- ¹⁶H. Daniel, H. Koch, G. Poelz, H. Schmitt, L. Tauscher, G. Backenstoss, and S. Charalambus, *Phys. Lett.* **26B**, 281 (1968).
- ¹⁷V. G. Zinov, A. D. Konin, and A. I. Mukhin, *Yad. Fiz.* **2**, 859 (1965) [*Sov. J. Nucl. Phys.* **2**, 613 (1966)].
- ¹⁸A. B. d'Oliveira, H. Daniel, and T. von Egidy, *Nuovo Cimento Lett.* **10**, 197 (1974).
- ¹⁹M. Y. Au-Yang and M. L. Cohen, *Phys. Rev.* **174**, 468 (1968).
- ²⁰L. C. Pauling, *The Nature of the Chemical Bond and the Structure of Molecules and Crystals* (Cornell U.P., Ithaca, New York, 1960), third edition.
- ²¹L. F. Mausner, R. A. Naumann, J. A. Monard, and S. N. Kaplan, *Phys. Lett.* **56B**, 145 (1975).
- ²²V. D. Bobrov, V. G. Varlamov, Yu. M. Grashin, B. A. Dolgoshein, V. G. Kirillov-Ugryumov, V. S. Roganov, A. V. Samoilov, and S. V. Somov, *Zh. Eksp. Teor. Fiz.* **48**, 1197 (1965) [*Sov. Phys.-JETP* **21**, 798 (1965)].
- ²³A. D. Konin, V. N. Pokrovsky, L. I. Ponomarev, H. Schneuwly, V. G. Zinov, and I. A. Yutlandov, *Phys. Lett.* **50A**, 57 (1974).
- ²⁴Yu. G. Budyashov, P. F. Ermolov, V. G. Zinov, A. D. Konin, and A. I. Mukhin, *Yad. Fiz.* **5**, 599 (1967) [*Sov. J. Nucl. Phys.* **5**, 426 (1967)].
- ²⁵G. Backenstoss, H. Daniel, K. Jentzsch, H. Koch, H. P. Povel, F. Schmeissner, K. Springer, and R. L. Stearns, *Phys. Lett.* **36B**, 422 (1971).
- ²⁶F. J. Hartmann, H. J. Pfeiffer, K. Springer, and H. Daniel, *Z. Phys.* **271**, 353 (1974).
- ²⁷D. Kessler, H. L. Anderson, M. S. Dixit, H. J. Evans, R. J. Mckee, C. K. Hargrove, R. D. Barton, E. P. Hincks, and J. D. McAndrew, *Phys. Rev. Lett.* **18**, 1179 (1967).
- ²⁸H. Daniel, H.-J. Pfeiffer, and K. Springer, *Phys. Lett.* **44A**, 447 (1973).